A Single-Phased Emission-Tunable Phosphor $Ca_9Y(PO_4)_7:Eu^{2+},Mn^{2+}$ with Efficient Energy Transfer for White-Light-Emitting Diodes

Chien-Hao Huang,[†] Teng-Ming Chen,*[,†] Wei-Ren Liu,[‡] Yi-Chen Chiu,[‡] Yao-Tsung Yeh,[‡] and Shyue-Ming Jang[‡]

Phosphors Research Laboratory and Department of Applied Chemistry, National Chiao Tung University, Hsinchu 30010, Taiwan, and Material and Chemical Research Laboratories, Industrial Technology Research Institute, Hsinchu 30011, Taiwan

ABSTRACT A series of single-composition emission-tunable $Ca_9Y(PO_4)_7:Eu^{2+},Mn^{2+}$ phosphors were synthesized by solid-state reaction. The energy transfer from Eu^{2+} to Mn^{2+} in $Ca_9Y(PO_4)_7$ host matrix was studied and demonstrated to be a resonant type via a dipole−quadrupole mechanism with the critical distance of ~ 11 Å. The wavelength-tunable white light can be realized by coupling the emission bands centered at 486 and 638 nm ascribed to the contribution from Eu^{2+} and Mn^{2+}, respectively. By properly tuning the relative composition of Eu^{2+}/Mn^{2+}, chromaticity coordinates of (0.31, 0.33) can be achieved under excitation at 250−440 nm. Moreover, white-light-emitting diodes were fabricated through the integration of 365 nm chips and single composition white-light-emitting phosphors $(Ca_{0.975}Eu_{0.01}Mn_{0.015})_9Y(PO_4)_7$ into a single package shows a cool white light of 7200 K, color rendering index of 76, and color coordinates of (0.30, 0.31) close to that of ideal white light can be achieved.

KEYWORDS: $Ca_9Y(PO_4)_7$ • Eu^{2+} • Mn^{2+} • photoluminescence • energy transfer • white-light LED

INTRODUCTION

In recent years, white-light-emitting diodes (LEDs) have attracted much attention due to their superior features as high efficiency, compactness, long operational lifetime, and environmental friendliness. Currently, white LEDs are widely used as daily lighting to replace conventional lighting sources such as incandescent and fluorescent lamps. There have been various combinations of phosphors and LEDs documented on the fabrication of white LEDs, namely (a) a blue InGaN LED chip and a YAG:Ce phosphor (1), (b) an UV LED chip and two, three, even four phosphors (2−4), and (c) an UV LED chip in combination with a single-composition white-light-emitting phosphors (5). Among various phosphor-converted (pc) white LED systems, the disadvantages of white LED by combining YAG:Ce and blue InGaN chip are poor color rendering index ($Ra < 80$) because of the lack of red-light contribution and also obstructs its extension for more vivid applications. In addition, it is also possible to produce white light by the means of adopting two, three, or even four phosphors (e.g., silicates and nitrides) with UV LED chips; poor luminous efficiency attributed to the reabsorption has commonly been encountered. Thus, a single-composition white-emitting phosphor is considered to be potentially useful because of small color aberration, high color rendering, and low cost. One of the strategies for generating white light from single-composition phosphors is by codoping sensitizer and activator into a crystalline matrix, using the principle of energy transfer (ET) from sensitizer to activator, such as Eu^{2+}/Mn^{2+}, which have been investigated in many hosts. For instance, $CaAl_2Si_2O_8$:Eu,Mn (5), $Ba_3MgSi_2O_8$:Eu,Mn (6), $BaMg_2Si_2O_7$:Eu,Mn (7), $MgCa_2Si_2O_7$:Eu,Mn (8), NaCl:Eu,Mn (9), NaBr:Eu,Mn (10), $CaCl_2$:Eu,Mn (11), $RbMgF_3$:Eu,Mn (12), $Ba_2Mg(BO_3)_2$:Eu,Mn (13), $Ca_5(PO_4)_3Cl$:Eu,Mn (14), $Sr_5(PO_4)_3Cl$:Eu,Mn (15), and $Sr_2P_2O_7$:Eu,Mn (16). The purpose of our study is to develop a interesting and versatile emission-tunable phosphor $Ca_9Y(PO_4)_7:Eu^{2+},Mn^{2+}$ (CYP:Eu^{2+},Mn^{2+}) that has not been reported in the literature.

Being isostructural with β-$Ca_9In(PO_4)_7$ (space group $R3c$, $Z = 6$) (17), the compound $Ca_9Y(PO_4)_7$ crystallizes in a rhombohedral (space group $R3c$ (No. 161)) cell with lattice constants of $a = 10.4442$ Å, $c = 37.324$ Å, $V = 3525.89$ nm^3, and $Z = 6$ and has seven crystallographically independent cation sites in the unit cell: two eight-coordinated Ca^{2+} site (Ca^{I}, Ca^{II}), one nine-coordinated Ca^{2+} site (Ca^{III}), one six-coordinated Y^{3+} site, and three four-coordinated P^{5+} sites. The ionic radii for eight- and nine-coordinated Eu^{2+} are 1.25 and 1.3 Å, respectively, and that for eight-coordinated Mn^{2+} is 0.96 Å. However, the ionic radii for eight- and nine-coordinated Ca^{2+} are 1.12 and 1.18 Å, respectively. Therefore, based on the effective ionic radii of cations with different coordination numbers, we have proposed that Eu^{2+} and Mn^{2+} are expected to randomly occupy the three Ca^{2+} sites in the host structure.

In this work, we report the preparation and investigation results on the luminescence and color chromaticity energy for a series of emission-tunable CYP:Eu^{2+},Mn^{2+} phosphors.

* Corresponding author. E-mail: tmchen@mail.nctu.edu.tw. Tel:+886-35731695.
Received for review October 5, 2009 and accepted December 17, 2009
[†] National Chiao Tung University.
[‡] Industrial Technology Research Institute.
DOI: 10.1021/am900668r

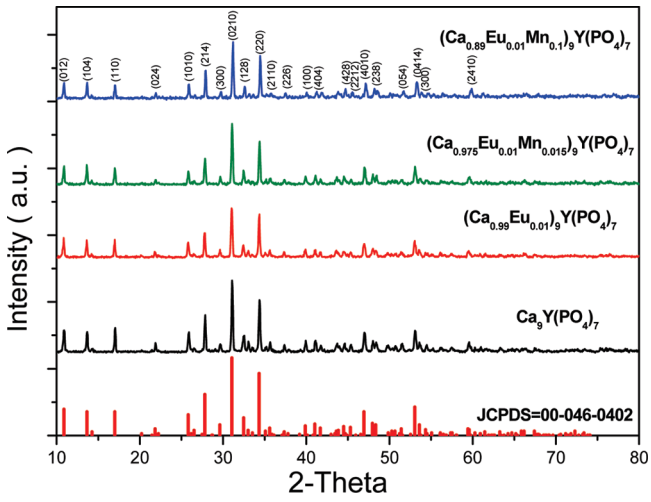

FIGURE 1. Powder XRD patterns of CYP, CYP:Eu, and CYP:Eu, Mn (JCPDS file no. 046−0402)

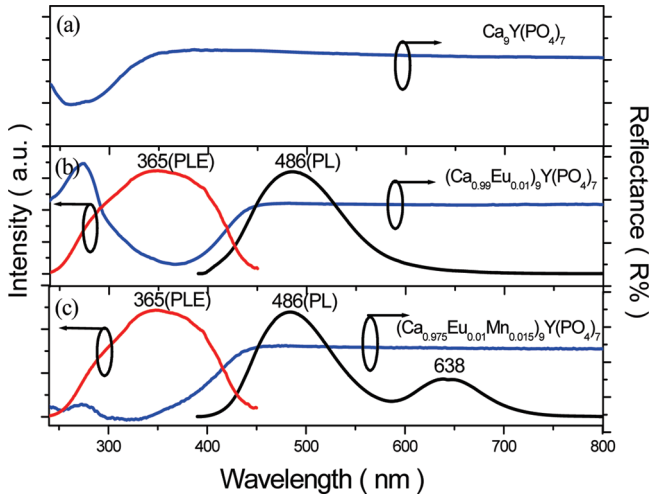

FIGURE 2. (a) Reflectance spectra of CYP. Reflectance and PL/PLE spectra of (b) CYP:0.01Eu^{2+} and (c) CYP:0.01Eu^{2+}, 0.015Mn^{2+} .

The mechanism and critical distance (R_c) for energy transfer from sensitizer Eu^{2+} to activator Mn^{2+} have also been determined. We have also successfully demonstrated the fabrication and packaging of a white pc-LED by adopting a white-emitting CYP:Eu^{2+},Mn^{2+} with an UV LED chip with wavelength of 365 nm.

EXPERIMENTAL SECTION

$Ca_9Y(PO_4)_7$:Eu^{2+},Mn^{2+} phosphors were synthesized by high-temperature solid-state reaction. The starting materials, $CaCO_3$ (A.R., 99.9%), Y_2O_3 (A.R., 99.99%), $(NH_4)_2HPO_4$ (Merck, ≥ 99%), Eu_2O_3 (A.R., 99.99%), and MnO (A.R., 99.9%), with stoichiometric molar ratios were thoroughly ground and mixed in an agate mortar, pressed into pellets and calcined at 1200 °C for 8 h. The obtained samples were then reduced at 1000 °C for 8 h under a reducing atmosphere of 40% H_2/60% Ar in an alumina boat. The crystal structure of the as-synthesized samples were identified by using powder X-ray diffraction analysis with a Bruker AXS D8 advanced automatic diffractometer with Cu Kα radiation. The photoluminescence (PL) and photoluminescence excitation (PLE) spectra of the samples were measured by using a Spex Fluorolog-3 Spectrofluorometer equipped with a 450 W Xe light source. The diffuse reflectance

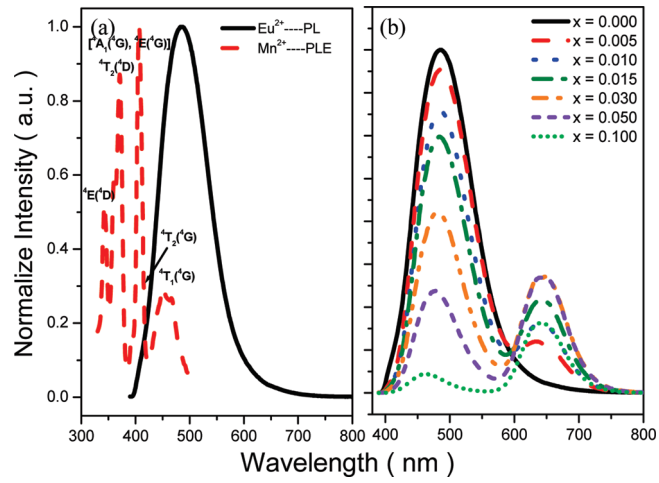

FIGURE 3. (a) Spectral overlap between PL spectrum of CYP:Eu^{2+} (solid line) and PLE spectrum of CYP:Mn^{2+} (dash line). (b) PL spectra of CYP:0.01Eu^{2+},xMn^{2+} phosphors (x = 0, 0.005, 0.01, 0.015, 0.03, 0.05, and 0.1) excited at 365 nm.

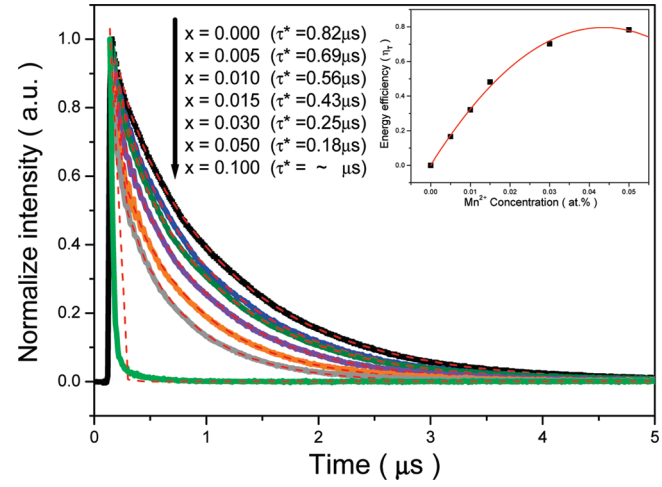

FIGURE 4. PL decay curves of the Eu^{2+} emission at 486 nm in CYP: 0.01Eu^{2+},xMn^{2+} (solid line) and curve-fitting (dash line) under excitation at 365 nm, monitored at 486 nm. The inset shows the η_T versus x relationship.

(DR) spectra were measured with a Hitachi 3010 double-beam UV−vis spectrometer (Hitachi Co., Tokyo, Japan). Time-resolved measurements were performed with a tunable nanosecond optical-parametric-oscillator/Q-switch-pumped YAG:Nd^{3+} laser system (NT341/1/UV, Ekspla). Emission transients were collected with a nanochromater (SpectraPro-300i, ARC), detected with photomultiplier tube (R928HA, Hamamatsu), connected to a digital oscilloscope (LT372, LeCrop) and transferred to a computer for kinetics analysis. The Commission International de l'Eclairage (CIE) chromaticity coordinates for all samples were measured by a Laiko DT-101 color analyzer equipped with a CCD detector (Laiko Co., Tokyo, Japan).

RESULTS AND DISCUSSION

The phase identification for CYP:Eu^{2+},Mn^{2+} samples characterized by XRD are portrayed as a profile shown in Figure 1. It was observed clearly that no detectable impurity phase was presented in CYP:Eu^{2+},Mn^{2+} even at high doping concentration of Eu^{2+} and Mn^{2+}. The XRD profiles were found to be in good agreement with that reported in JCPDS file No. 046−0402 (18). These results indicated that the codopant of Eu^{2+}/Mn^{2+} in CYP retains to be single phase.

Table 1. Decay Lifetime for Exponential Components of CYP:0.01Eu^{2+},xMn^{2+} Phosphors Excited at 365 nm with the Emission Monitored at 486 nm

sample	τ_1	A_1	τ_2	A_2	τ^* (μs)[a]
$x = 0.000$	1.47×10^{-7}	0.350	1.06×10^{-6}	1.010	0.82
$x = 0.005$	1.37×10^{-7}	0.451	9.43×10^{-7}	0.963	0.69
$x = 0.010$	1.24×10^{-7}	0.728	9.07×10^{-7}	0.910	0.56
$x = 0.015$	9.88×10^{-8}	1.048	8.23×10^{-7}	0.863	0.43
$x = 0.030$	7.43×10^{-8}	2.140	7.09×10^{-7}	0.790	0.25
$x = 0.050$	6.88×10^{-8}	2.771	5.82×10^{-7}	0.761	0.18
$x = 0.100$	3.08×10^{-8}	96.71	-1.23×10^{137}	0.001	

[a] τ^* (effective time constant) $= (A_1\tau_1^2 + A_2\tau_2^2)/(A_1\tau_1 + A_2\tau_2)$.

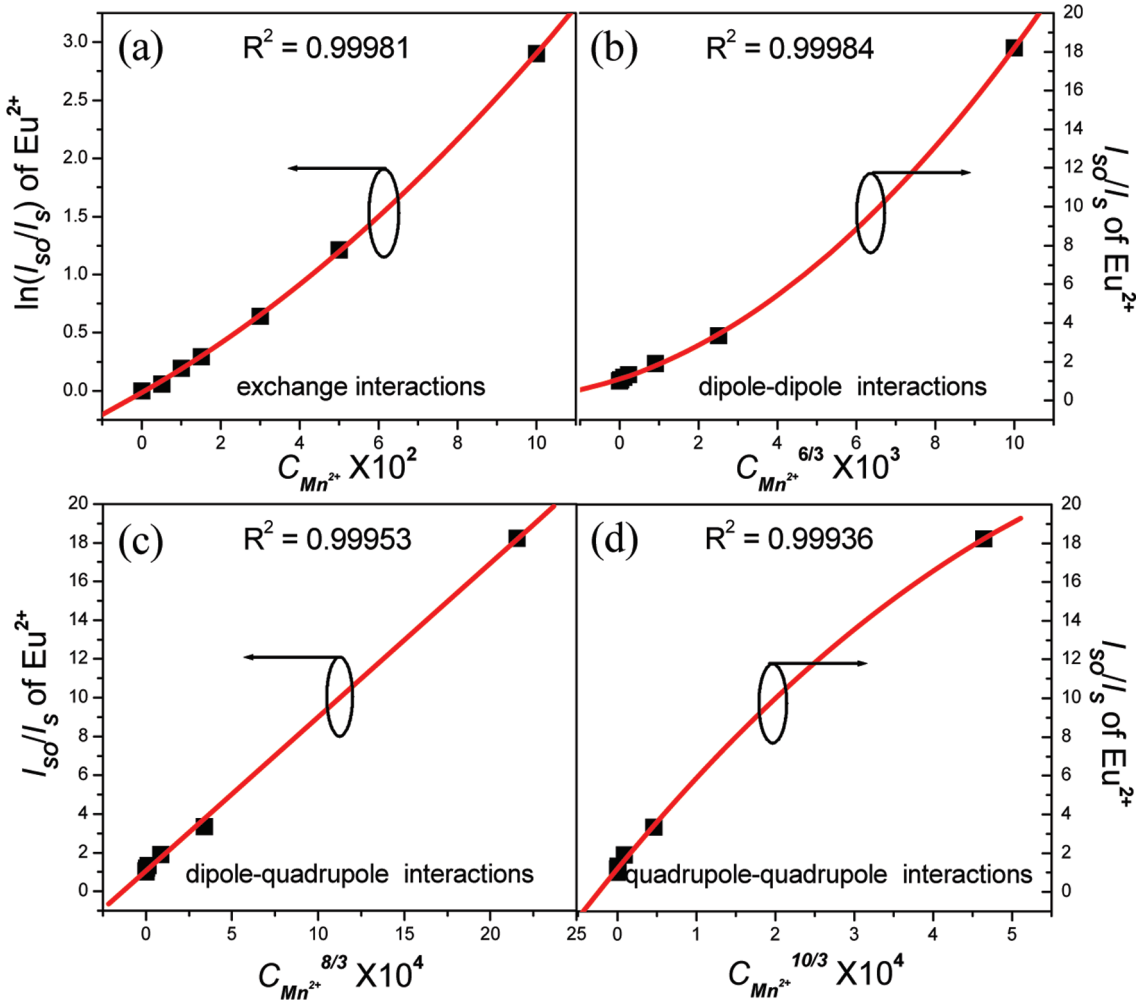

FIGURE 5. (a) Dependence of $\ln(I_{S0}/I_S)$ of Eu^{2+} on C_{Mn2+}; and I_{S0}/I_S of Eu^{2+} on (b) $C_{Mn2+}^{6/3}$;(c) $C_{Mn2+}^{8/3}$ and (d) $C_{Mn2+}^{10/3}$.

Figure 2a−c illustrate the reflection and PL/PLE spectra of CYP, CYP:Eu^{2+}, and CYP:Eu^{2+},Mn^{2+}, respectively. The optimization of Eu^{2+} dopant concentration for $Ca_9Y(PO_4)_7$:Eu^{2+} revealed that the optimal dopant content was 1%. Therefore, the concentration of Eu^{2+} of CYP:0.01Eu^{2+},xMn^{2+} was fixed at 0.01 for all samples. The CYP host material shows an energy absorption in the ≤340 nm region (Figure 2a). The reflection spectra of CYP and CYP:Eu^{2+}, and CYP:Eu^{2+},Mn^{2+} were different, which a strong absorption in the 250−440 nm near-UV range was observed not only for CYP:0.01Eu^{2+} (Figure 2b), but also for CYP:0.01Eu^{2+},0.015Mn^{2+} (Figure 2(c)). The PLE spectra (λ_{em} = 486 nm) showed a broad hump between 250 to 440 nm, which was consistent with that observed in the reflection spectrum. The PL spectra (λ_{ex} = 365 nm) of CYP:Eu^{2+} showed a broad blue-greenish emission. On the other hand, the CYP:Eu^{2+},Mn^{2+} exhibited two broad blue-greenish and red emission bands centering at 486 and at 638 nm ($^4T_1$ (^4G) → $^6A_1$ (^6S) transition of Mn^{2+}), respectively. The broad and symmetric emission bands of CYP:Eu^{2+} and CYP:Mn^{2+} may be attributed to the transitions of Eu^{2+} and Mn^{2+} occupying three crystallographically distinct Ca^{2+} sites in the host structure.

As presented in Figure 3a, the effective resonance energy transfer was expected from Eu^{2+} to Mn^{2+} based on the

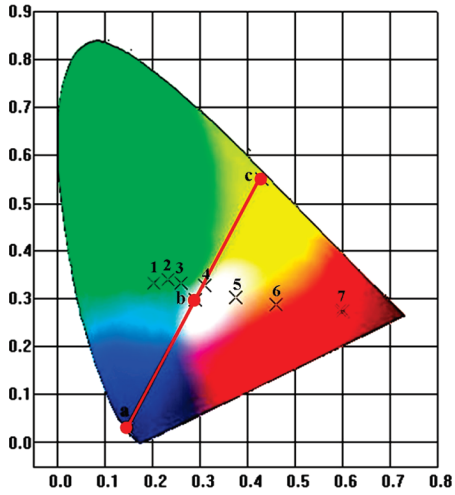

FIGURE 6. CIE chromaticity diagram for CYP:0.01Eu^{2+},xMn^{2+} excited at 365 nm. (1) $x = 0$; (2) $x = 0.005$; (3) $x = 0.01$; (4) $x = 0.015$; (5) $x = 0.03$; (6) $x = 0.05$; (6) $x = 0.1$.

Table 2. Comparison of CIE Chromaticity Coordinates for CYP:0.01Eu^{2+},xMn^{2+} ($\lambda_{ex} = 365$ nm) and Simulated White Light Using $Y_3Al_5O_{12}$:Ce^{3+} Commodity ($\lambda_{ex} = 460$ nm)

no. point in CIE diagram	samples	CIE (x, y)
1	$x = 0.000$	(0.203, 0.335)
2	$x = 0.005$	(0.233, 0.342)
3	$x = 0.010$	(0.261, 0.334)
4	$x = 0.015$	(0.310, 0.330)
5	$x = 0.030$	(0.376, 0.305)
6	$x = 0.050$	(0.460, 0.290)
7	$x = 0.100$	(0.597, 0.278)
a	blue InGaN chip from Nichia	(0.144, 0.030)
b	white light $Y_3Al_5O_{12}$:Ce^{3+}	(0.291, 0.300)
c	$Y_3Al_5O_{12}$:Ce^{3+} commodity	(0.429, 0.553)

observed significant spectral overlap between the emission band centered at 486 nm of CYP:Eu^{2+} (solid line) and the excitation band centered at 450 nm of CYP:Mn^{2+} (dashed line). The PL spectrum showed an intense emission broadband centered at 486 nm, which was assigned to the $4f^65d^1 \rightarrow 4f^7$ transition of CYP:Eu^{2+}. The PLE spectrum of CYP:Mn^{2+} contained of several bands centered at 343, 372, 407, 418, and 450 nm, corresponding to the transitions from the $^6A_1$ (^6S) to ^4E (^4D), $^4T_2$ (^4D), [$^4A_1$ (^4G), ^4E (^4G)], $^4T_2$ (^4G), and $^4T_1$ (^4G) levels, respectively. Therefore, the effective resonance-type $ET_{Eu\rightarrow Mn}$ was expected. Figure 3b shows PL spectra of CYP:0.01Eu^{2+},xMn^{2+} ($x = 0$, 0.005, 0.01, 0.015, 0.03, 0.05, and 0.1). The PL emission intensity at 486 nm of Eu^{2+} decreased with the increasing Mn^{2+} content x, and the emission intensity of Mn^{2+} at 638 nm was found to increase with increasing Mn^{2+} content x until the appearance of concentration quenching in Mn^{2+} content of 0.05, which further supported the occurrence of the energy transfer from Eu^{2+} to Mn^{2+}. Moreover, similar phenomenon was observed and discussed by Ruelle et al. (19). The possible rationalization could be attributed to the formation of paired Mn^{2+} centers with faster decay than single Mn^{2+} centers.

As shown in Figure 4, the PL decay curves of the Eu^{2+} emission at 486 nm of CYP:0.01Eu^{2+},xMn^{2+} phosphors was obtained under the excitation at 365 nm, monitored at 486 nm. The corresponding luminescent decay times can be calculated by a curve-fitting (Figure 4 dash line) technique according to the following equation (20)

$$I = A_1\exp(-t/\tau_1) + A_2\exp(-t/\tau_2) \quad (1)$$

where I is the luminescence intensity; A_1 and A_2 are constants; t is the time, and τ_1 and τ_2 are decay time for exponential. The values of τ_1 and τ_2 are summarized and compared in Table 1; the results show that τ_1 and τ_2 decrease with increasing doped Mn^{2+} content x. The effective time constant (τ^*) were determined to be 0.82, 0.69, 0.56, 0.43, 0.25, and 0.18 μs for CYP:0.01Eu^{2+},xMn^{2+} with $x = 0$, 0.005, 0.01, 0.015, 0.03, and 0.05, respectively. In particular, the decay lifetime of CYP:0.01Eu^{2+},0.1Mn^{2+} was too short and beyond the detection limit of our instruments.

The inset in Figure 4 displays the relationship between energy transfer efficiency (η_T) and concentration of Mn^{2+}. The energy transfer efficiency (η_T) can be expressed by Paulose et al.(21)

$$\eta_T = 1 - \frac{\tau_S}{\tau_{S0}} \quad (2)$$

where τ_{S0} is the lifetime of the sensitizer Eu^{2+} of the sample in the absence of Mn^{2+}, and τ_s is the lifetime of Eu^{2+} in the presence of Mn^{2+}. As a consequence, the η_T from Eu^{2+} to Mn^{2+} in CYP:0.01Eu^{2+},xMn^{2+} was calculated as a function of x and is represented in the inset of Figure 4. With increasing Mn^{2+} dopant content, the η_T was observed to increase and reach the saturation when x is above 0.0455.

According to Dexter's energy transfer formula for exchange and multipolar interactions, the following relation can be obtained (22, 23)

$$\ln\left(\frac{I_{S0}}{I_S}\right) \propto C \quad (3)$$

$$\frac{I_{S0}}{I_S} \propto C^{\alpha/3} \quad (4)$$

where C is the concentration of Mn^{2+}; I_{S0} and I_S are the luminescence intensities of the sensitizer (Eu^{2+}) with and without activator (Mn^{2+}) present, respectively. $\ln(I_{S0}/I_S) \propto C$ corresponds to the exchange interaction and $(I_{S0}/I_S) \propto C^{\alpha/3}$ with $\alpha = 6$, 8, and 10 corresponds to dipole−dipole, dipole−quadrupole, and quadrupole−quadrupole interactions, respectively. The relationships of $\ln(I_{S0}/I_S) \propto C$ and $(I_{S0}/I_S) \propto C^{\alpha/3}$ are illustrated in Figure 5, which a linear behavior was observed only when $\alpha = 8$, implying that energy transfer from Eu^{2+} to Mn^{2+} occurs via a dipole−quadrupole mechanism, which is similar to those previously investigated and observed in our group.

Furthermore, the expression for the dipole−quadrupole transfer probability (W_{sa}^{DQ}) is represented by (11)

$$W_{sa}^{DQ} = \frac{3\hbar^4c^4f_q\lambda_s^2Q_a}{4\pi n^4\tau_s^0f_dR_{sa}^8}\Omega(F_s,F_a) \quad (5)$$

where τ_s^o is the intrinsic lifetime of sensitizer, f_d and f_q are the oscillator strengths of the activator dipole and quadrupole electrical transitions, λ_s is the emission wavelength of the sensitizer Eu^{2+}, Q_a is the integrated absorption coefficient

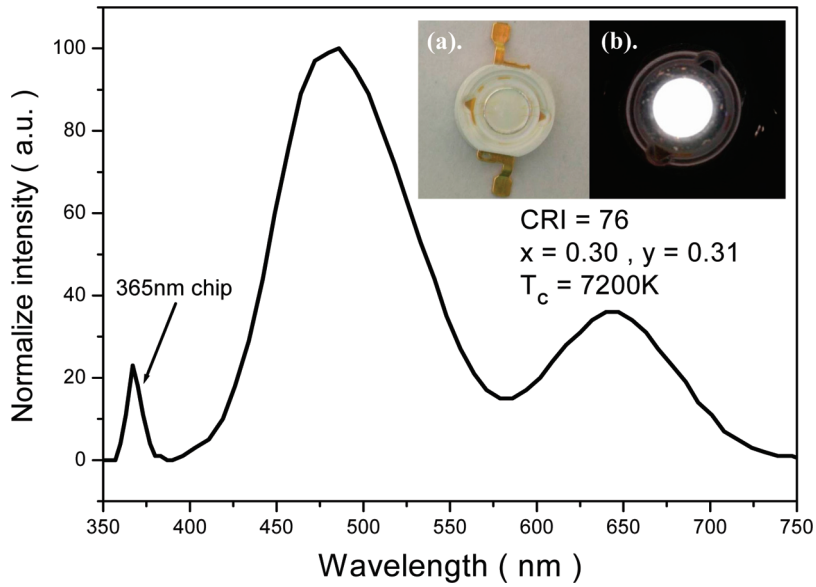

FIGURE 7. EL spectrum of a pc-LED lamp fabricated with a 365 nm LED chip and a white-emitting phosphor CYP:0.01Eu^{2+},0.015Mn^{2+}, driven by 350 mA current.

of Mn^{2+} the acceptor; $\hbar$, η c, π, and n are constants, R_{sa} is the distance between the ions involved in the transfer, and $\Omega(F_s, F_a) = \int F_s(E)F_a(E)E^{-4}dE$ represents the spectral overlap between the normalized Eu^{2+} emission $F_s(E)$ and Mn^{2+} absorption $F_a(E)$; this is shown in Figure 3 and was estimated to be about 3.09×10^{-2} eV^{-5}.

The critical distance (R_c) for energy transfer from Eu^{2+} to Mn^{2+} is defined as the distance at which the energy transfer rate is equal to the radiative emission rate of the sensitizer, i.e., $W_{sa}^{DQ}\tau_s^o = 1$. Therefore, R_c for a dipole−quadrupole type energy transfer can be calculated according to the following equation (6, 23)

$$R_c^8 = 0.63 \times 10^{28} \frac{f_q \lambda_s^2 Q_a}{f_d E_s^4} \int F_s(E)F_a(E)dE \qquad (6)$$

where $Q_a = 4.8 \times 10^{-16}$, f_d is the absorption coefficient of Mn^{2+}; $f_d = 1 \times 10^{-7}$ and $f_q = 1 \times 10^{-10}$ are the oscillator strengths of dipole and quadrupole electrical transitions for Mn^{2+}; λ_s (in Å) and E_s (in eV) are the emission wavelength and emission energy of Eu^{2+}, and $\int F_s(E)F_a(E)dE$ expresses the spectral overlap between the Eu^{2+} and Mn^{2+}, and it was estimated be 1.31 eV^{-1}. In this system, the critical distance of energy transfer was calculated to be 11.04 Å.

The CIE chromaticity diagram for the CYP: 0.01Eu^{2+},xMn^{2+} phosphors with different x values were measured and shown in Figure 6. The color tone or hue can be tuned from blue-greenish, represented by point 1 (solely 0.01Eu^{2+}) through white and eventually to red, represented by point 7 (0.01Eu^{2+}/0.1Mn^{2+}), corresponding to chromaticity coordinates (x, y) varying from (0.203, 0.335) to (0.597, 0.278). The chromaticity variation with different Eu^{2+}/Mn^{2+} ratio is also summarized in Table 2.

Consequently, white light with a variety of hues can be generated by adjusting the Mn^{2+} content (x), in particular, we have demonstrated white light with (0.31, 0.33) can be achieved in CYP:0.01Eu^{2+},0.015Mn^{2+}. The white light produced by combination of YAG:Ce whose chromaticity coordinates are (0.457, 0.529) and blue-LED chip with (0.144, 0.030), and experimentally determined chromaticity coordinates is found to be (0.291, 0.300) for the simulated white light (24).

Table 3. Full Set of the 14 CRIs and the *Ra* of a Single-Phased CYP:0.01Eu^{2+},0.015Mn^{2+} Phosphor Excited at 365 nm

	R1	*R2*	*R3*	*R4*	*R5*	*R6*	*R7*	*R8*	*R9*	*R10*	*R11*	*R12*	*R13*	*R14*	*Ra*
CYP:Eu,Mn	90	75	63	75	91	71	69	75	36	42	82	78	74	89	76

The electroluminescence (EL) spectrum of a phosphor converted (pc)-LED lamp fabricated with a 365 nm UV LED chip and a white-emitting CYP:0.01Eu^{2+},0.015Mn^{2+} and driven with a 350 mA current is shown in Figure 7. Correlated color temperature was determined to be 7200 K and the CIE color coordinates were (0.30, 0.31). The average color-rendering index $Ra = 76$ is given in Table 3.

However, as indicated in Table 3, the color rendering index ($Ra = 76$) of the white LED based on a single-phased CYP:0.01Eu^{2+},0.015Mn^{2+} phosphor and pumped with 365 nm UV chip was observed to be significantly higher than that ($Ra = 71$) of a LED based on YAG:Ce with blue InGaN chip (25), because of the lack of red light contribution. The inset in Figure 7a shows the appearance of the phosphor-converted white LED lamp and Figure 7b shows the white light emission from the LED driven by a 350 mA current. Our LED packaging results demonstrate that CYP:Eu^{2+},Mn^{2+} is a great potential and flexible candidate by choosing the blending ratio of the UV-excitable white-emitting phosphors. The inset shows the appearance of a well-packaged three-phosphor-converted-LED lamp in operation.

CONCLUSIONS

In summary, we have synthesized a series of novel emission-tunable $Ca_9Y(PO_4)_7$:Eu^{2+},Mn^{2+} phosphors by solid-state reaction. The energy transfer from Eu^{2+} to Mn^{2+} in $Ca_9Y(PO_4)_7$:Eu^{2+},Mn^{2+} has been investigated. The results are

consistent with an electric dipole−quadrupole interaction and the critical distance was simultaneously calculated to be ~11.04 Å. Moreover, a white LED was also fabricated through the integration of a 365 nm UV chip and a single-phased white-light phosphor $(Ca_{0.975}Eu_{0.01}Mn_{0.015})_9Y(PO_4)_7$ and showed that a cool white light with color temperature of 7200 K, *Ra* of 76, and color coordinates of (0.30, 0.31). These results indicate that the performance of a white pc-LED with $(Ca_{0.975}Eu_{0.01}Mn_{0.015})_9Y(PO_4)_7$ is superior to that of white YAG:Ce^{3+} pc-LED pumped with a blue LED chip in color rendering property.

Acknowledgment. This research was supported by National Science Council of Taiwan (ROC) under Contract NSC98-2113-M-009-005-MY3 (T.M C.) and, in part, by Industrial Technology Research Institute (C.-H.H.) under Contract 8301XS1751.

REFERENCES AND NOTES

(1) Schlotter, P.; Schmide, R. *Appl. Phys., A* **1997**, *64*, 417.
(2) Kim, J. S.; Kang, J. Y.; Jeon, P. E.; Choi, J. C.; Park, H. L.; Kim, T. W *Jpn. J. Appl. Phys., Part 1* **1992**, *31*, 2786.
(3) Wu, H.; Zhang, X.; Guo, C.; Xu, J.; Wu, M.; Su, Q. *IEEE Photonics Technol. Lett.* **2005**, *17*, 1160.
(4) Lee, S. H.; Park, J. H.; Son, S. M.; Kim, J. S.; Park, H. L. *Appl. Phys. Lett.* **2006**, *89*, 221916.
(5) Yang, W. J.; Luo, L.; Chen, T. M.; Wang, N. S. *Chem. Mater.* **2005**, *17*, 3883.
(6) Kim, J. S.; Lim, K. T.; Jeong, Y. S.; Jeon, P. E.; Choi, J. C.; Park, H. L. *Solid State Commun.* **2005**, *135*, 21.
(7) Yao, G. Q.; Lin, J. H.; Zhang, L.; Lu, G. X.; Gong, M. L.; Su, M. Z. *J. Mater. Chem.* **1998**, *8*, 585.
(8) Chang, C. K.; Chen, T. M. *Appl. Phys. Lett.* **2007**, *90*, 161901.
(9) Rubio, J. O.; Muñoz, A. F.; Muñoz, G. H. *J. Phys. C: Solid State Phys.* **1988**, *21*, 2059.
(10) Rubio, J. O. *Phys. Rev. B* **1984**, *39*, 3834.
(11) Caldiño, U. G.; Muñoz, A. F.; Rubio, J. O. *J. Phys.: Condens. Matters* **1993**, *5*, 2195.
(12) Shinn, M. D.; Sibley, W. A. *Phys. Rev. B* **1984**, *29*, 3834.
(13) Yuan, S.; Yang, Y.; Zhang, X.; Tessier, F.; Cheviré, F.; Adam, J. L.; Moine, B.; Chen, G. *Opt. Lett.* **2008**, *33*, 2865.
(14) Setlur, A. A.; Shiang, J. J.; Happek, U. *Appl. Phys. Lett.* **2008**, *92*, 081104.
(15) Guo, C.; Luan, L.; Ding, X.; Zhang, F.; Shi, F. G.; Gao, F.; Liang, L. *Appl. Phys. B: Laser Opt.* **2009**, *95*, 779.
(16) Ye, S.; Liu, Z. S.; Wang, J. G.; Jing, X. P. *Mater. Res. Bull.* **2008**, *43*, 1057.
(17) Morozov, V. A.; Belik, A. A.; Stefanovich, S. Y.; Grebenev, V. V.; Lebedev, O. I.; Van Tendeloo, G.; Lazoryak, B. I. *J. Solid State Chem.* **2002**, *165*, 278.
(18) JCPDS file no. 00−046−0402.
(19) Ruelle, N.; Pham-Thi, M.; Fouassier, C. *Jpn. J. Appl. Phys.* **1992**, *31*, 2786.
(20) Pang, R.; Li, C.; Shi, L.; Su, Q. *J. Phys. Chem. Solids* **2009**, *70*, 303.
(21) Paulose, P. I.; Jose, G.; Thomas, V.; Unnikrishnan, N. V.; Warrier, M. K. R. *J. Phys. Chem. Solids* **2003**, *64*, 841.
(22) Dexter, D. L. *J. Chem. Phys.* **1953**, *21*, 836.
(23) Blass, G. *Philips Res. Rep.* **1969**, *24*, 131.
(24) Chiang, C. C.; Tsai, M. S.; Hon, M. H. *J. Alloys Compd.* **2007**, *431*, 298.
(25) Jang, H. S.; Im, W. B.; Lee, D. C.; Jeon, D. Y.; Kim, S. S. *J. Lumin.* **2007**, *126*, 371.

AM900668R